Soil Bulk Density and Matric Potential Regulate Soil CO$_2$ Emissions by Altering Pore Characteristics and Water Content

Weiyang Gui [1], Yongliang You [2], Feng Yang [3] and Mingjun Zhang [4],*

[1] Key Laboratory of Animal Genetics, Breeding and Reproduction in the Plateau Mountainous Region, Ministry of Education, College of Animal Science, Guizhou University, Guiyang 550025, China
[2] Dryland Farming Institute, Hebei Academy of Agricultural and Forestry Sciences, Hengshui 053000, China
[3] Guizhou Grassland Technology Experiment and Extension Station, Guiyang 550025, China
[4] Livestock and Poultry Genetic Resources Management Station of Guizhou Province, Guiyang 550025, China
* Correspondence: mingjunzhang23@163.com

Abstract: Soil pore structure and soil water content are critical regulators of microbial activity and associated carbon dioxide (CO$_2$) emissions. This study evaluated the impacts of soil bulk density and matric potential on carbon dioxide (CO$_2$) emissions through modifications of total porosity, air-filled porosity, water retention, and gas diffusivity. Soil samples were manipulated into four bulk densities (1.0, 1.1, 1.2, and 1.3 Mg m^{-3}) and ten matric potential levels (-1, -2, -3, -4, -5, -6, -7, -8, -9, and -10 kPa) in controlled soil cores. The results showed that lower bulk densities enhanced while higher densities suppressed CO$_2$ emissions. Similarly, wetter matric potentials decreased fluxes, but emission increased with drying. Correlation and regression analyses revealed that total porosity (r = 0.28), and gravimetric water content (r = 0.29) were strongly positively related to CO$_2$ emissions. In contrast, soil bulk density (r= -0.22) and matric potential (r= -0.30) were negatively correlated with emissions. The results highlight that compaction and excessive water content restrict microbial respiration and gas diffusion, reducing CO$_2$ emissions. Proper management of soil structure and water content is therefore essential to support soil ecological functions and associated ecosystem services.

Keywords: soil bulk density; matric potential; CO$_2$ emissions; pore characteristics; soil moisture content

1. Introduction

Soil respiration, characterized by the emissions of carbon dioxide (CO$_2$) from the soil surface, encapsulates both plant root and microbial respiration, making it a valuable indicator of soil carbon (C) cycling [1]. Elevated atmospheric CO$_2$ levels, regarded as a principal greenhouse gas, not only aggravate global climate change but also manipulate the carbon stores and soil water content in terrestrial ecosystems, potentially causing escalated CO$_2$ emissions. This cycle suggests a positive feedback loop, thereby heightening the urgency for CO$_2$ emission mitigation, especially considering the growing rates of atmospheric CO$_2$ concentrations [2].

The emission of soil CO$_2$, chiefly driven by production and transportation processes, relates to the interchange of oxygen and CO$_2$ between soil and atmosphere. Soil respiration includes both oxygen depletion and CO$_2$ production [3]. Here, soil diffusivity emerges as a vital factor influencing oxygen availability and CO$_2$ transport from soil to the surrounding environment [4]. It is important to note that soil diffusivity is associated with both soil porosity and water content [4,5]. Various studies have proposed equations linking CO$_2$ and soil water content; however, these fail to express the physical force of water held in soil or soil pore connectivity and tortuosity [3,6].

Matric potential serves as a robust indicator of water availability to plant roots and microbes [3,7,8], yet many studies have overlooked soil bulk density when investigating the matric potential effect on CO$_2$ [9–11]. A more effective predictor of soil gas emissions like

nitrous oxide or nitrogen is relative gas diffusivity (D_p/D_o), which adjusts for variations in soil water content and soil bulk density [12–15]. However, research on this aspect in relation to soil CO_2 emission remains scant [16].

A majority of studies have calculated D_p/D_o through measuring soil porosity or water content or through model assessments due to the challenges in directly measuring soil gas diffusivity [4,5,14,17,18]. The relationship between D_p/D_o and soil porosity can vary with changes in total porosity or the continuity of soil pores due to differences in soil bulk density or water content [5,17]. Soil bulk density affects the available pore space for gas diffusion, with higher densities leading to compaction and reduced porosity [19]. Similarly, variations in water content can either fill or empty pore spaces, affecting the continuity of the pores and subsequently the gas diffusion process [15,20,21]. These changes in physical properties are essential as they govern microbial activity, nutrient cycling, and plant growth, collectively impacting the overall functionality and health of the soil ecosystem [3]. Consequently, directly measuring D_p/D_o rather than relying on empirical equations or models provides a more accurate understanding of these critical soil processes. Understanding the effects of variations in bulk density and matric potential on soil diffusivity will enhance our understanding of the control mechanisms governing soil sources and sinks of atmospheric gases.

This study aims to examine the interaction between soil bulk density and matric potential on D_p/D_o and CO_2 emissions, focusing on uncovering the underlying mechanisms in specific soil types (Ali-Perudic Argosols). By directly measuring these parameters and exploring their intricate relationships across different levels of bulk density and matric potential, the study intends to provide new insights that may have broader implications for soil management practices and climate-change-mitigation strategies. Specifically, the objective was to quantify how soil D_p/D_o and CO_2 emissions respond across a range of bulk densities and matric potentials in controlled soil cores. We hypothesized that D_p/D_o will serve as an effective indicator of soil CO_2 emissions under diverse bulk density and matric potential conditions.

2. Materials and Methods

2.1. Soil Collection, Experimental Design, and Setup

Soil was randomly sampled (0–15 cm) from Dafang County (27°23′ N, 105°52′ E; Altitude 1760 m), Bijie City, Guizhou Province (Figure 1) in June 2023 and then was air-dried. The soil carbon, nitrogen, and soil pH were measured before experimenting (Table 1). The composition of soil aggregates and particles within a depth of 0–10 cm was measured before the experiment (Table 2).

Table 1. Mean soil organic carbon (SOC, g kg^{-1}), total (TN, g kg^{-1}) and available nitrogen, total and available phosphorus (TP, AP, g kg^{-1}), and total potassium (TK, g kg^{-1}) at 0–5 and 5–10 cm in the study region.

Soil Layer (cm)	SOC (g·kg^{-1})	TN (g·kg^{-1})	Nitrate N (mg·kg^{-1})	Ammonium N (mg·kg^{-1})	TP (g·kg^{-1})	AP (mg·kg^{-1})	TK (g·kg^{-1})
0–5	27.05	2.82	23.14	4.95	0.80	24.08	27.75
5–10	24.46	2.59	16.83	5.06	0.66	14.99	28.79

Table 2. Basic soil aggregates and particle composition of soil depth (0–10 cm) before experiment.

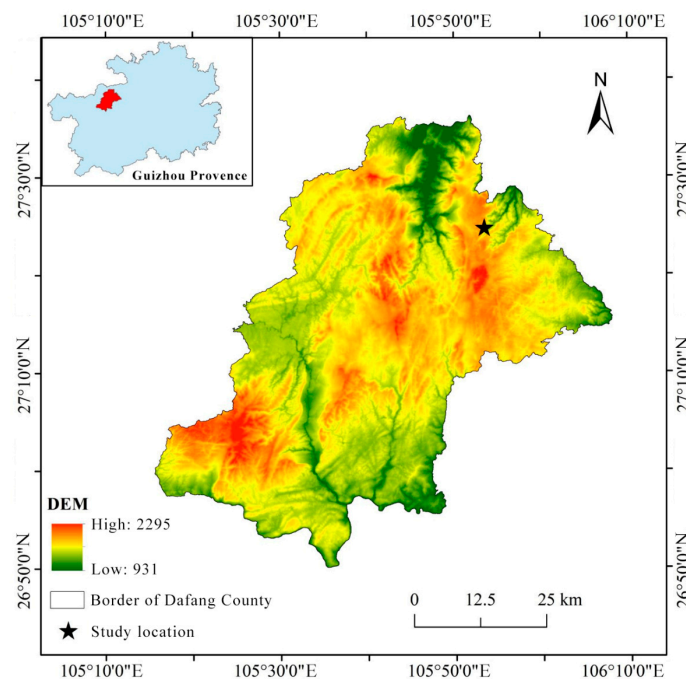| Index		Soil Aggregates Composition (%)			Soil Particle Composition (%)		
					Clay	Silt	Sand
Layer (cm)	5–2 mm	2–0.25 mm	0.25–0.053 mm	<0.053 mm	<0.002 mm	0.002–0.02 mm	0.02–2 mm
0–5	0.34	0.43	0.09	0.11	24.35	61.09	14.56
5–10	0.38	0.41	0.09	0.08	26.58	60.50	12.92

Figure 1. Study location in southeast China.

The main soil type is Ali-Perudic Argosols (APA) according to the International Society of Soil Sciences standards. After the soil was sieved (≤ 2 mm), soil cores were made by compacting soil into stainless-steel cylinders (7.3 cm internal diameter, 7.4 cm deep) to obtain four levels of bulk density (1.0, 1.1, 1.2, and 1.3 Mg m^{-3}). Bulk density was measured using the core method, where the dry weight of a known volume of soil was determined. Each bulk density level had ten levels of matric potential (-1, -2, -3, -4, -5, -6, -7, -8, -9, and -10 kPa) measured using tensiometers at varying depths, and the entire process was replicated four times. The soil cores were preincubated for 7 days to stabilize the microbial activity [12,13].

2.2. Soil CO$_2$ Emissions and Relative Gas Diffusivity Measurements

To measure the soil CO$_2$ emissions, the soil cores were taken off the tension tables and placed into 1 L stainless-steel tins equipped with gas-tight lids pre-fitted with rubber septa. Soil CO$_2$ emissions were measured on days 4, 5, and 6.

According to the method of Rolston and Moldrup [20], we measured soil D$_p$/D$_o$ after measuring CO$_2$ flux: a chamber containing a calibrated oxygen sensor was purged with a gas mixture (90% Ar and 10% N$_2$), while the base of the soil core was isolated from the chamber. Once the chamber oxygen concentration equaled 0%, the base of the soil core was exposed to the oxygen-free chamber atmosphere. As oxygen diffused through the soil core into the chamber, the change in oxygen concentration was recorded as a function of time over a period of 120 to 180 min. It was assumed that any error in the measured value of D$_p$ due to oxygen consumption was negligible [20]. Regression analysis of the log-plot of relative oxygen concentration vs. time enabled D$_p$ (oxygen diffusion coefficient in soil) to be calculated [20]. All diffusivity calculations were performed at 25 °C, and the value of D$_o$ (oxygen diffusion coefficient in air) at 25 °C was calculated to be 0.074 m^2 h^{-1} [22].

2.3. Soil Analyses and Calculations

Soil gravimetric water content (θ_g) was measured by drying 10 g wet soil subsamples at 105 °C for 24 h. Soil air-filled porosity (ε), total porosity (φ), volumetric water content (θ_v), and water-filled pore space (*WFPS*) were calculated by using values of soil bulk density (ρ_d) (Equations (1)–(4)) while assuming a particle density (ρ_b) of 2.65 Mg m^{-3} [3].

$$\theta_v = \rho_b \times \theta_g \tag{1}$$

$$\Phi = 1 - \frac{\rho_b}{\rho_d} \tag{2}$$

$$\varepsilon = \Phi - \theta_v \tag{3}$$

$$WFPS = \frac{\theta_V}{\Phi} \tag{4}$$

2.4. Data Analyses

The effects of bulk density and matric potential on soil pore characteristics and soil CO_2 emissions were tested using analysis of variance (ANOVA) in the "agricolae" package of R version 1.3.1 [23]. Principal component analysis (PCA) was conducted to examine multivariate relationships and clustering by bulk density and observation days. Pearson's correlation analysis quantified correlation coefficients between all measured variables. Statistically significant effects were declared at $p < 0.05$. All analyses were performed in R statistical software (version 1.3.1). Prior to analysis, data normality and homogeneity of variance were confirmed using the Shapiro–Wilk test and Levene's test, respectively. Figures were constructed with the ggplot2 package in R.

3. Results

3.1. Impact of Changes in Soil Bulk Density and Matric Potential on Soil Pore Characteristics

As bulk density increased from 1.0 to 1.3 Mg m^{-3}, total porosity decreased from 0.63 to 0.52 m^3 m^{-3} (overall mean, $p < 0.01$; Figure 2). A similar decline was observed in air-filled porosity (from 0.26 to 0.07 m^3 m^{-3}) with increasing bulk density ($p < 0.01$). Conversely, volumetric water content and water-filled pore space showed an opposite trend, increasing from 0.37 to 0.46 m^3 m^{-3} and from 0.58 to 0.89 m^3 m^{-3}, respectively, as bulk density increased ($p < 0.01$). Gravimetric water content was relatively stable across the bulk densities, and the highest values (0.39 g g^{-1}) appeared with bulk density of 1.1 Mg m^{-3} ($p < 0.01$). Nonetheless, relative gas diffusivity exhibited a sharp decrease from 0.029 to 0.001 with higher bulk density ($p < 0.01$).
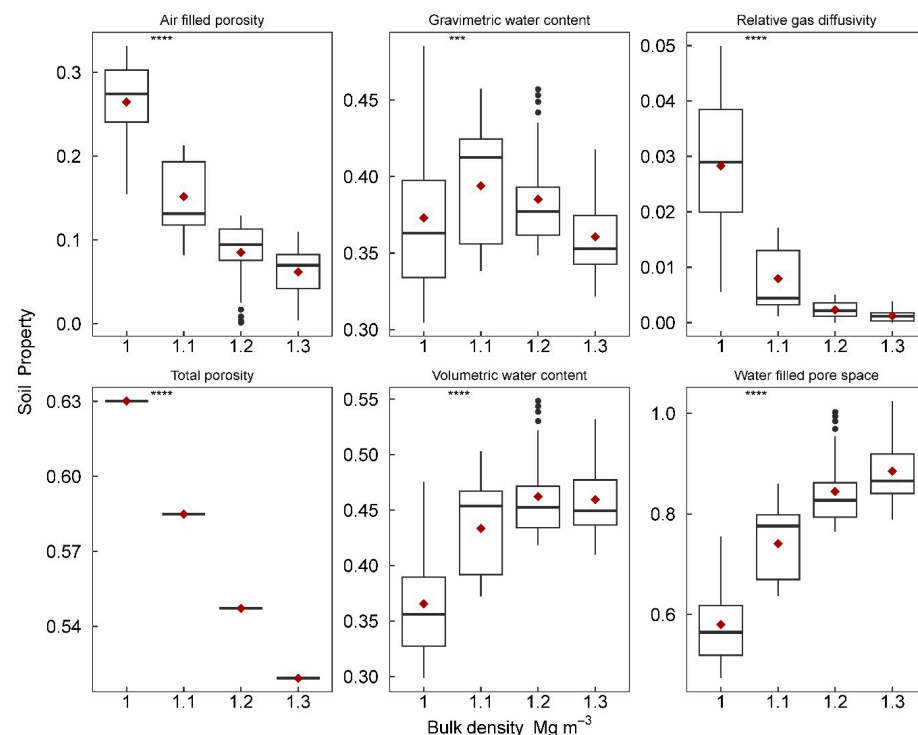

Figure 2. Soil air-filled porosity, gravimetric water content, relative gas diffusivity, total porosity, volumetric water content, and water-filled pore space in response to changes in soil bulk density.

Treatments include four levels of bulk density (1.0, 1.1, 1.2, and 1.3 Mg m^{-3}), and each bulk density has ten levels of matric potential (-1, -2, -3, -4, -5, -6, -7, -8, -9, and -10 kPa). Notes: The significance indicates the differences with *** $p < 0.001$ and **** $p < 0.0001$. Red dot indicates mean values.

Changes in the matric potential affected soil pore characteristics (Figure 3). As matric potential increased from -10 to -1 kPa, volumetric water content decreased from 0.52 to 0.38 m^3 m^{-3} ($p < 0.01$). Similarly, gravimetric water content and water-filled pore space significantly declined from 0.45 to 0.33 g g^{-1} and from 0.88 to 0.63 m^3 m^{-3}, respectively, with decreasing matric potential. In contrast, air-filled porosity increased from 0.06 to 0.19 m^3 m^{-3} with lower matric potential ($p < 0.01$), while relative gas diffusivity increased from 0.001 to 0.018 as matric potential decreased ($p < 0.01$).
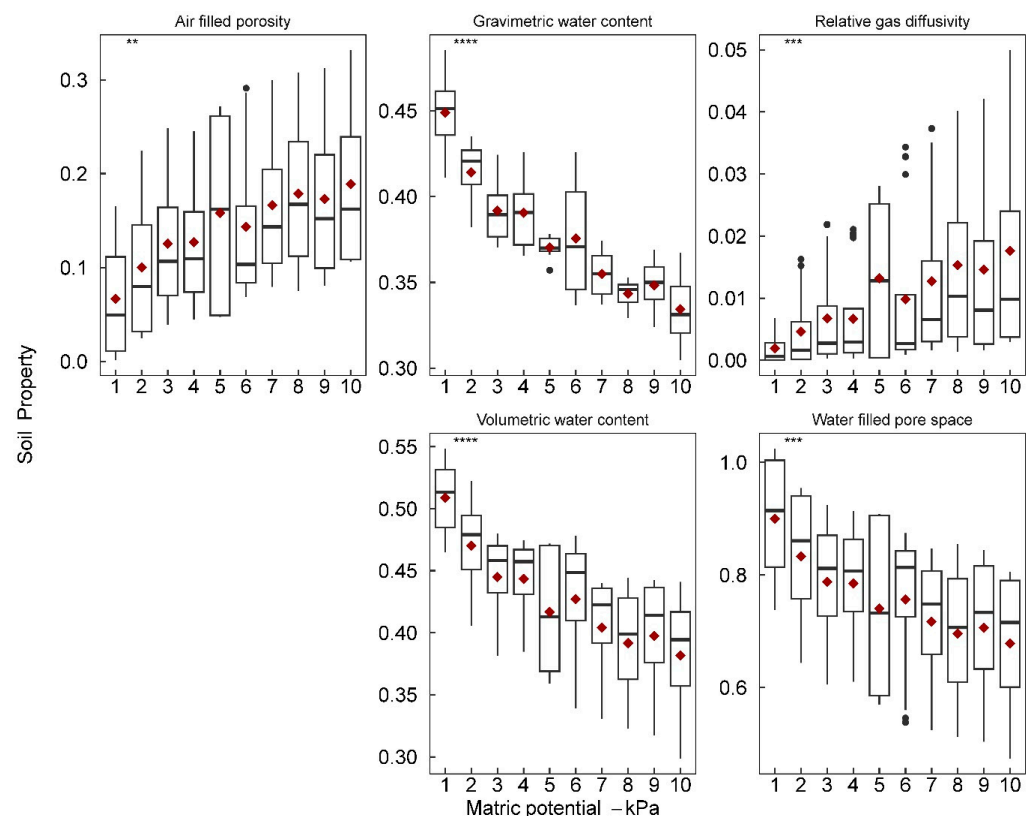

Figure 3. Soil air-filled porosity, gravimetric water content, relative gas diffusivity, total porosity, volumetric water content, and water-filled pore space in response to changes in soil matric potentials. Treatments include four levels of bulk density (1.0, 1.1, 1.2, and 1.3 Mg m^{-3}), and each bulk density has ten levels of matric potential (-1, -2, -3, -4, -5, -6, -7, -8, -9, and -10 kPa). Notes: The significance indicates the differences with ** $p < 0.01$, *** $p < 0.001$ and **** $p < 0.0001$. Red dot indicates mean values.

3.2. Soil CO$_2$ Emissions in Response to Changes in Soil Bulk Density and Matric Potential

Soil CO$_2$ emissions across varying soil bulk densities were monitored over 3 days (Figure 4). On day 4, soil CO$_2$ emissions ranged from 4.2 to 7.1 mol m^{-2} s^{-1} (overall mean) across the bulk densities. Soil CO$_2$ emissions were lowest in the bulk density treatment of 1.3 Mg m^{-3} and highest in the low-density treatment (1.0 Mg m^{-3}, $p < 0.01$). A similar trend was observed on day 5. By day 6, soil CO$_2$ emissions declined.
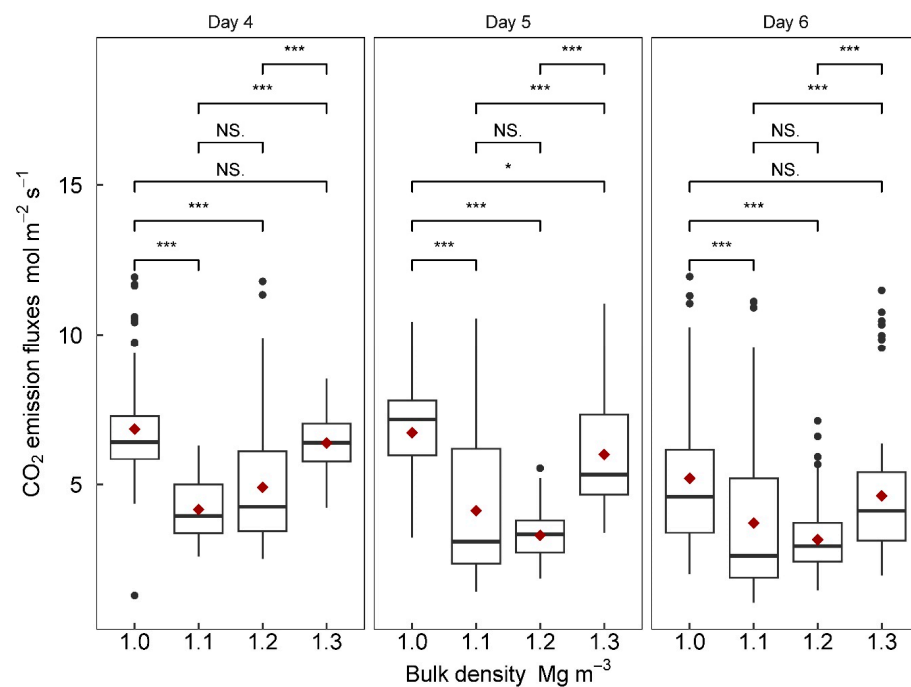
Figure 4. Soil carbon dioxide (CO_2) emissions with four levels of soil bulk density over three days. Notes: The significance indicates the differences with * $p < 0.05$ and *** $p < 0.001$. Red dot indicates mean values.

The effects of matric potential on soil CO_2 emissions were also evaluated over three days (Figure 5). On day 4, soil CO_2 emissions were lowest at −10 kPa matric potential around 4.9 mol m^{-2} s^{-1} and increased to 6.4 mol m^{-2} s^{-1} at −5 kPa matric potential. A similar trend was observed on day 5, and soil CO_2 emissions peaked at −5 kPa matric potential, with a value of 9.1 mol m^{-2} s^{-1}. By day 6, fluxes declined slightly across all matric potentials, with the decline more pronounced at low potentials (−7 to −10 kPa); however, soil CO_2 emissions peaked at −5 kPa matric potential again, with value of 10.3 mol m^{-2} s^{-1}.
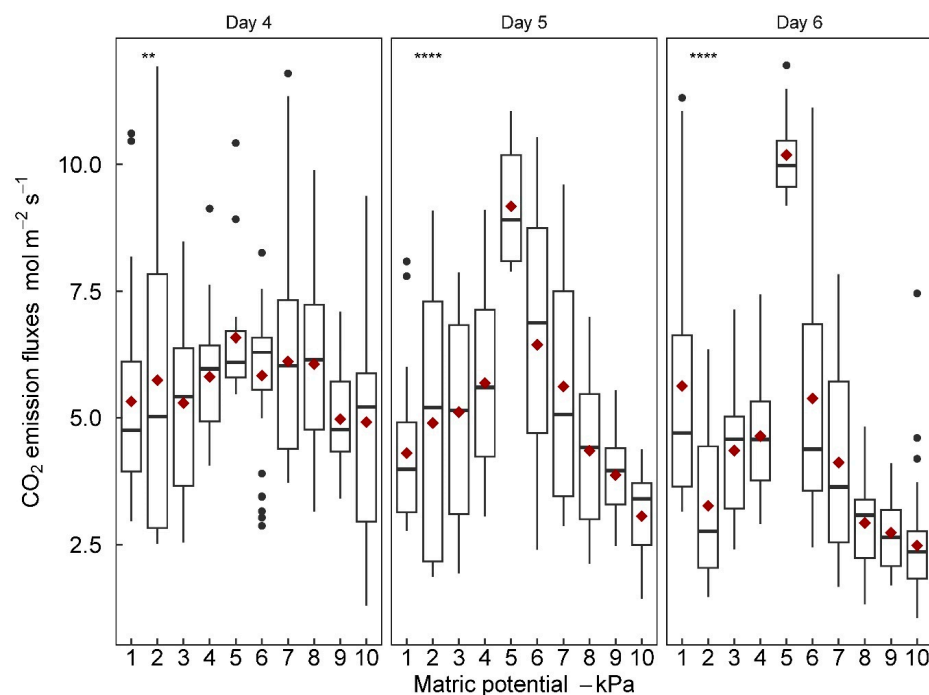

Figure 5. Soil carbon dioxide (CO_2) emissions with ten levels of soil matric potentials over three days. Notes: The significance indicates the differences with ** $p < 0.01$ and **** $p < 0.0001$. Red dot indicates mean values.

The PCA showed a slight separation of the four bulk density levels along the first principal component (44.2% variance explained; Figure 6). However, it did not present distinct clustering of the three measurement days along PC1 (43.2% variance explained).
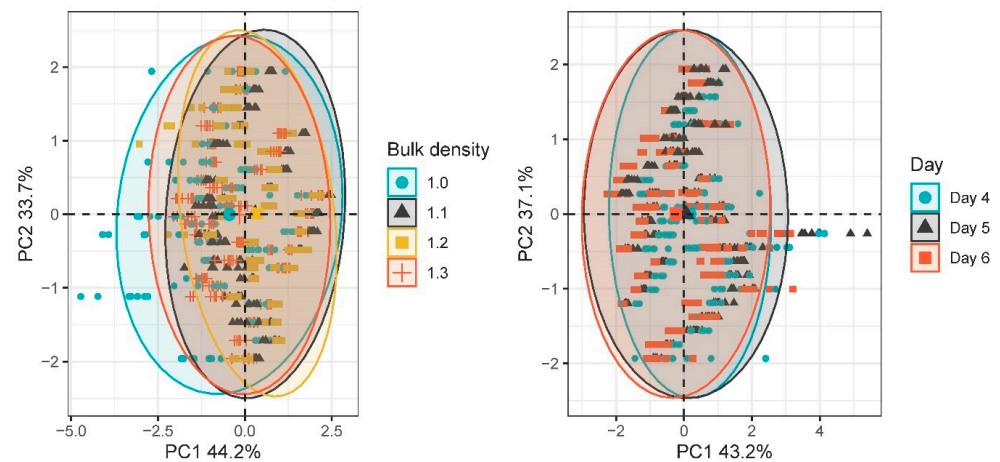

Figure 6. Principal component analysis (PCA) for soil carbon dioxide (CO_2) emissions at different bulk densities or measuring time (day). The different shapes indicate different bulk densities or measuring times, and the ellipse is the confidence interval of the distribution of variables under different treatments.

3.3. Factors Affecting Soil CO_2 Emissions in Various Bulk Densities and Matric Potentials

Distribution of soil CO_2 emissions under various soil pore characteristics was illustrated (Figure 7), and the relationships between soil CO_2 emissions and gravimetric water content and volumetric water content were significant (Table 3). Soil gravimetric water content and volumetric water content explained 43% and 36% of the variations of soil CO_2 emissions ($p < 0.01$).
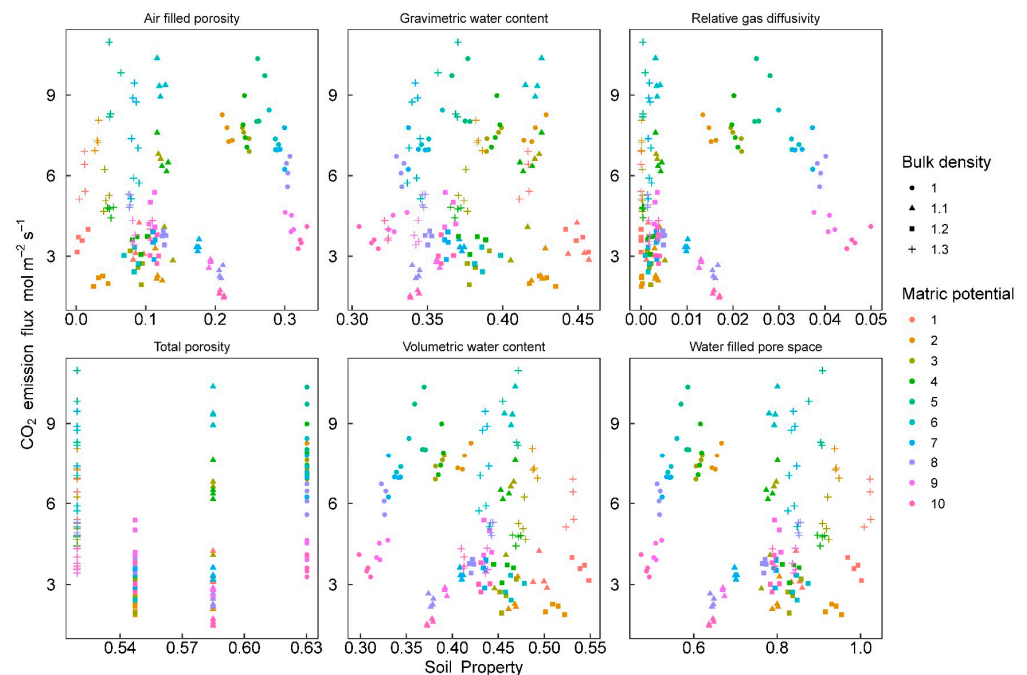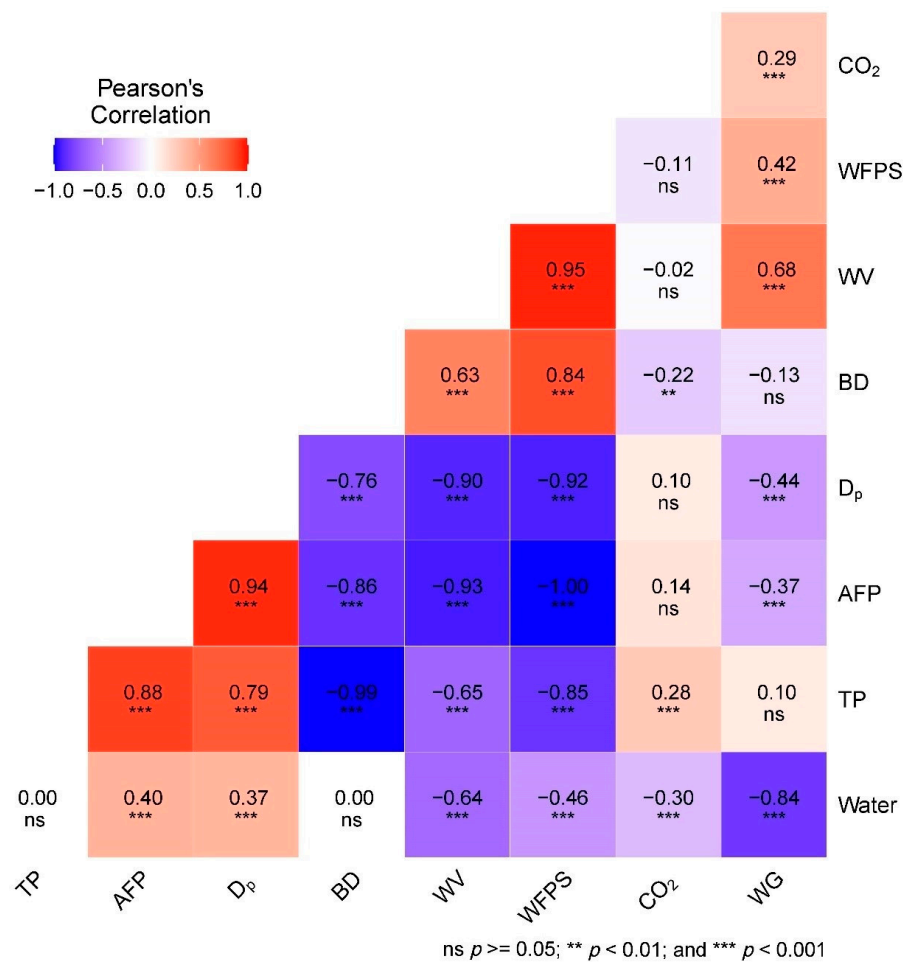

Figure 7. The desaturations of soil carbon dioxide (CO_2) emissions with air-filled porosity, gravimetric water content, relative gas diffusivity, total porosity, volumetric water content, and water-filled pore space over three days. Treatments include four levels of bulk density (1.0, 1.1, 1.2, and 1.3 Mg m^{-3}), and each bulk density has ten levels of matric potential (-1, -2, -3, -4, -5, -6, -7, -8, -9, and -10 kPa).

Table 3. The regression of soil carbon dioxide (CO_2) emissions with gravimetric water content and volumetric water content over three days.

Soil Property	Equation	R^2	p
Gravimetric water content	$y = 0.0009x^2 - 0.16x + 10.41$	0.43	<0.01
Volumetric water content	$y = 0.0009x^2 - 0.15x + 9.96$	0.36	<0.01

A Pearson's correlation analysis was conducted to assess relationships between the soil pore characteristics and soil CO_2 emissions (Figure 8). Significant positive correlations were observed between soil CO_2 emissions and total porosity (r = 0.28) and between soil CO_2 emissions and gravimetric water content (r = 0.29), while significant negative correlations were observed between soil CO_2 emissions and matric potential (r = −0.30) and bulk density (r = −0.22).

Figure 8. Correlation analysis of factors affecting soil carbon dioxide (CO_2) emissions in response to air-filled porosity (AFP), gravimetric water content (WG), relative gas diffusivity (Dp), total porosity (TP), volumetric water content (TP), and water-filled pore space (WFPS) over three days. Notes: The significance indicates the differences with ** $p < 0.01$ and *** $p < 0.001$.

4. Discussion

The observed reduction in total porosity and air-filled porosity with a rise in bulk density aligns with previous research, suggesting that greater soil compaction leaves less pore space [24–27]. This compaction is accompanied by reductions in volumetric water content and water-filled pore space, echoing the decreased overall porosity. Meanwhile, the minimal change in gravimetric water content indicates a roughly consistent total water mass, albeit one that occupies a smaller volume due to compaction. In contrast, relative gas

diffusivity sharply declines, reflecting a significant decrease in gas diffusion and transport capacity due to the reduced air-filled porosity at higher bulk densities [22,25]. These observations reinforce the significant influence of bulk density on soil pore characteristics and associated properties, underscoring the need for careful soil bulk density management to maintain optimal conditions for water availability [28], aeration, and gas diffusion.

Increased volumetric water content and water-filled pore space with decreasing matric potential can be attributed to greater water retention and the displacement of air by water as pores become more saturated at increasingly negative water potentials [29]. Similarly, the rise in gravimetric water content suggests a higher absolute water mass within the soil pores due to the greater water retention potential. Concurrently, the pronounced reduction in relative gas diffusivity reflects the decrease in air-filled porosity given that lower diffusivity corresponds to severely hampered gas diffusion through saturated pores [30]. These trends illustrate how matric potential can fundamentally alter pore water retention dynamics, aeration, and gas transport, underscoring the importance of proper irrigation management to maintain optimal matric potential for plant growth, soil ecological function, and greenhouse gas transport.

Lower soil CO_2 emissions at higher bulk densities likely reflect significantly reduced microbial activity and gas diffusion due to compaction [31,32]. The highest fluxes occur in less-compacted, low-density soils, which provide more ideal conditions for microbial processes and gas diffusion. Soil CO_2 emissions increasing over time in high-density soil suggests a chronic constraint on microbial activity and gas diffusion [24,33], with diffusion pathways gradually opening over time to release previously trapped soil CO_2. These data emphasize that soil compaction can severely reduce soil CO_2 emissions, impacting microbial respiration, carbon cycling, and climate regulation ecosystem services negatively [34–36]. Hence, maintaining sufficient soil porosity is crucial for preserving microbial function and soil health [2].

Lower fluxes under wet conditions reflect constrained diffusion and decreased oxygen availability for aerobic respiration. As soil progressively dries, diffusion pathways open, alleviating oxygen limitation and enabling higher microbial activity and soil CO_2 production [10]. The fluxes' general decline by day 6 might be due to the depletion of labile carbon substrates under the constant wetting and drying cycles, emphasizing the sensitivity of soil CO_2 emissions to soil water content and the need to balance adequate water content for microbial activity without oversaturation [10,37].

The PCA suggests that bulk density and measurement day were key factors influencing soil CO_2 emissions. The non-overlapping clusters of bulk density treatments indicate that changes in pore structure from soil compaction significantly impact gas fluxes, including reduced microbial activity and constrained diffusion [24,38]. The temporal shifts in fluxes over the days reflect the dynamic nature of microbial activity and water contents, emphasizing the critical consideration of bulk density management and monitoring timeframe in experiments and data interpretation on soil CO_2 emissions.

Positive correlations between soil CO_2 emissions and total porosity, air-filled porosity, and gas diffusivity highlight the importance of diffusion pathways and oxygen availability for aerobic microbial metabolism and gas transport [3,20,26,38]. As pores become saturated, oxygen limitation restricts soil CO_2 production and diffusion, hence the negative correlations with volumetric water content and water-filled pore space. While gravimetric water content affects respiration substrate availability, its weaker correlation indicates that physical factors enabling gas transport predominantly control it. Although the results did not fully support our hypothesis that relative gas diffusivity would correspond as an indicator of how compaction and water retention influence soil CO_2 emissions, the data suggest a threshold effect where soil CO_2 emissions changed dramatically at certain levels of compaction and matric potential (Figure 7). In our analysis, we noted that the regression coefficients (R^2) were relatively low in some instances. There are several factors that could contribute to these lower R^2 values: (1) Complex interactions: Soil properties such as bulk density and matric potential interact with each other and with other unmeasured variables

in intricate ways. This complexity may not be fully captured by the models used, leading to a lower R^2. (2) It is worth noting that a low R^2 does not necessarily mean that the model is inadequate. R^2 only explains the proportion of variance captured by the model, and in complex ecological systems, it might not be realistic to expect a very high R^2. In future studies, more sophisticated modeling techniques that can account for non-linearities, interactions, and spatial patterns might be employed to possibly increase the R^2 values. Additionally, expanding the study to include more variables or more extensive sampling might help in understanding the underlying mechanisms more accurately.

From a broader perspective, this research contributes compelling evidence that the effective management of physical structure and moisture characteristics is integral to regulating soil CO_2 emissions. The insights gained from these findings have significant implications for enhancing soil functionality and may guide agricultural practices that align with climate regulation ecosystem services. Extending this research to include studies involving different types of soils and various management practices could further enrich our understanding, as soil bulk density and matric potential effects may vary across diverse soil ecosystems. Future investigations could delve into the interactive impacts of soil biological communities, organic matter, and mineralogy on soil CO_2 emissions, as seen in conjunction with soil structure. Additionally, field monitoring of emissions across diverse management gradients, including different soil types and cultivation methods, can offer further insights into the dynamic nature of soil CO_2 emissions. This research acts as a stepping stone to a deeper understanding of the intricate relationships between soil characteristics and greenhouse gas emissions, with direct implications for climate-change-mitigation strategies. The inclusion of different soil types and management practices in future studies will provide a more comprehensive picture, enhancing our ability to develop effective strategies for various agricultural contexts.

5. Conclusions

The findings of this study, conducted on Ali-Perudic Argosols (APA), highlight the pivotal role of physical structure and soil water characteristics in the regulation of soil CO_2 emissions. Within this specific soil type, total porosity, air-filled pore space, and gas diffusivity are seen as key contributors that facilitate microbial activity and CO_2 diffusion when conditions are optimal. Nevertheless, emissions are severely limited by pore saturation and compaction, which underline the criticality of maintaining suitable soil structure and soil water content for optimal soil health and functionality. These conclusions are directed explicitly at the soil type studied, and additional research on various soil types may further generalize these findings.

References

1. Raich, J.W.; Schlesinger, W.H. The global carbon dioxide flux in soil respiration and its relationship to vegetation and climate. *Tellus Ser. B-Chem. Phys. Meteorol.* **1992**, *44*, 81–99. [CrossRef]
2. Atmospheric CO_2 Growth Rates, Decadal Average Annual Growth Rates. Available online: https://gml.noaa.gov/ccgg/trends/gl_gr.html (accessed on 17 June 2023).

3. Linn, D.M.; Doran, J.W. Effect of water-filled pore space on carbon dioxide and nitrous oxide production in tilled and nontilled soils. *Soil Sci. Soc. Am. J.* **1984**, *48*, 1267–1272. [CrossRef]
4. Davidson, E.A.; Trumbore, S.E. Gas diffusivity and production of CO_2 in deep soils of the eastern Amazon. *Tellus Ser. B-Chem. Phys. Meteorol.* **1995**, *47*, 550–565. [CrossRef]
5. Millington, R.J. Gas Diffusion in Porous Media. *Science* **1959**, *130*, 100–102. [CrossRef] [PubMed]
6. Farquharson, R.; Baldock, J. Concepts in modelling N_2O emissions from land use. *Plant Soil* **2008**, *309*, 147–167. [CrossRef]
7. Liu, F.; Zhu, Q.; Wang, Y.; Lai, X.; Liao, K.; Guo, C. Storages and leaching losses of soil water dissolved CO_2 and N_2O on typical land use hillslopes in southeastern hilly area of China. *Sci. Total Environ.* **2023**, *886*, 163780. [CrossRef]
8. Vremec, M.; Forstner, V.; Herndl, M.; Collenteur, R.; Schaumberger, A.; Birk, S. Sensitivity of evapotranspiration and seepage to elevated atmospheric CO_2 from lysimeter experiments in a montane grassland. *J. Hydrol.* **2023**, *617*, 128875. [CrossRef]
9. Davidson, E.A.; Verchot, L.V.; Cattanio, J.H.; Ackerman, I.L.; Carvalho, J.E.M. Effects of soil water content on soil respiration in forests and cattle pastures of eastern Amazonia. *Biogeochemistry* **2000**, *48*, 53–69. [CrossRef]
10. Li, Z.; Cui, S.; Zhang, Q.; Xu, G.; Feng, Q.; Chen, C.; Li, Y. Optimizing Wheat Yield, Water, and Nitrogen Use Efficiency With Water and Nitrogen Inputs in China: A Synthesis and Life Cycle Assessment. *Front. Plant Sci.* **2022**, *13*, 930484. [CrossRef]
11. Orchard, V.A.; Cook, F.J. Relationship between soil respiration and soil moisture. *Soil Biol. Biochem.* **1983**, *15*, 447–453. [CrossRef]
12. Balaine, N.; Clough, T.J.; Beare, M.H.; Thomas, S.M.; Meenken, E.D. Soil gas diffusivity controls N_2O and N_2 emissions and their ratio. *Soil Sci. Soc. Am. J.* **2016**, *80*, 529–540. [CrossRef]
13. Balaine, N.; Clough, T.J.; Beare, M.H.; Thomas, S.M.; Meenken, E.D.; Ross, J.G. Changes in relative gas diffusivity explain soil nitrous oxide flux dynamics. *Soil Sci. Soc. Am. J.* **2013**, *77*, 1496–1505. [CrossRef]
14. Owens, J.; Clough, T.J.; Laubach, J.; Hunt, J.E.; Venterea, R.T.; Phillips, R.L. Nitrous oxide fluxes, soil oxygen, and denitrification potential of urine- and non-urine-treated soil under different irrigation frequencies. *J. Environ. Qual.* **2016**, *45*, 1169–1177. [CrossRef] [PubMed]
15. Rolston, D.E.; Moldrup, P. Gas Diffusivity. In *Methods of Soil Analysis: Part 4 Physical Methods*; Topp, G.C., Dane, J.H., Eds.; SSSA: Madison, WI, USA, 2002; pp. 1113–1139.
16. Räty, M.; Termonen, M.; Soinne, H.; Nikama, J.; Rasa, K.; Järvinen, M.; Lappalainen, R.; Auvinen, H.; Keskinen, R. Improving coarse-textured mineral soils with pulp and paper mill sludges: Functional considerations at laboratory scale. *Geoderma* **2023**, *438*, 116617. [CrossRef]
17. Fang, C.; Moncrieff, J.B. A model for soil CO_2 production and transport 1: Model development. *Agric. For. Meteorol.* **1999**, *95*, 225–236. [CrossRef]
18. Abeysinghe, A.M.S.N.; Lakshani, M.M.T.; Amarasinghe, U.D.H.N.; Li, Y.; Deepagoda, T.C.; Fu, W.; Fan, J.; Yang, T.; Ma, X.; Clough, T.; et al. Soil-gas diffusivity-based characterization of variably saturated agricultural topsoils. *Water* **2022**, *14*, 2900. [CrossRef]
19. Du, Y.; Guo, S.; Wang, R.; Song, X.; Ju, X. Soil pore structure mediates the effects of soil oxygen on the dynamics of greenhouse gases during wetting–drying phases. *Sci. Total Environ.* **2023**, *895*, 165192. [CrossRef]
20. Moldrup, P.; Olesen, T.; Gamst, J.; Schjønning, P.; Yamaguchi, T.; Rolston, D.E. Predicting the gas diffusion coefficient in repacked soil: Water-induced linear reduction model. *Soil Sci. Soc. Am. J.* **2000**, *64*, 1588–1594. [CrossRef]
21. Jiang, J.; Gu, K.; Xu, J.; Li, Y.; Le, Y.; Hu, J. Effect of Barometric Pressure Fluctuations on Gas Transport over Soil Surfaces. *Land* **2023**, *12*, 161. [CrossRef]
22. Currie, J.A. Gaseous diffusion in porous media Part 1. A non-steady state method. *Br. J. Appl. Phys.* **1960**, *11*, 314–317. [CrossRef]
23. Mendiburu, F.D. Statistical Procedures for Agricultural Research. R Package Version 1.3.1. 2009. Available online: https://CRAN.R-project.org/package=agricolae (accessed on 17 June 2023).
24. da Silva, T.S.; Pulido-Moncada, M.; Schmidt, M.R.; Katuwal, S.; Schlüter, S.; Köhne, J.M.; Mazurana, M.; Juhl Munkholm, L.; Levien, R. Soil pore characteristics and gas transport properties of a no-tillage system in a subtropical climate. *Geoderma* **2021**, *401*, 115222. [CrossRef]
25. Eden, M.; Schjønning, P.; Moldrup, P.; De Jonge, L.W. Compaction and rotovation effects on soil pore characteristics of a loamy sand soil with contrasting organic matter content. *Soil Use Manag.* **2011**, *27*, 340–349. [CrossRef]
26. Li, Y.; Li, Z.; Cui, S.; Jagadamma, S.; Zhang, Q. Residue retention and minimum tillage improve physical environment of the soil in croplands: A global meta-analysis. *Soil Tillage Res.* **2019**, *194*, 104292. [CrossRef]
27. Schjønning, P.; Munkholm, L.J.; Moldrup, P.; Jacobsen, O.H. Modelling soil pore characteristics from measurements of air exchange: The long-term effects of fertilization and crop rotation. *Eur. J. Soil Sci.* **2002**, *53*, 331–339. [CrossRef]
28. Qin, W.F.; Zhao, X.C.; Yang, F.; Chen, J.H.; Mo, Q.S.; Cui, S.; Chen, C.; He, S.J.; Li, Z. Impact of fertilization and grazing on soil N and enzyme activities in a karst pasture ecosystem. *Geoderma* **2023**, *437*, 116578. [CrossRef]
29. Wolf, A.B.; Vos, M.; de Boer, W.; Kowalchuk, G.A. Impact of Matric Potential and Pore Size Distribution on Growth Dynamics of Filamentous and Non-Filamentous Soil Bacteria. *PLoS ONE* **2014**, *8*, 83661. [CrossRef]
30. Killham, K.; Amato, M.; Ladd, J.N. Effect of substrate location in soil and soil pore-water regime on carbon turnover. *Soil Biol. Biochem.* **1993**, *25*, 57–62. [CrossRef]
31. Li, Y.; Clough, T.J.; Moinet, G.Y.K.; Whitehead, D. Emissions of nitrous oxide, dinitrogen and carbon dioxide from three soils amended with carbon substrates under varying soil matric potentials. *Eur. J. Soil Sci.* **2021**, *72*, 2261–2275. [CrossRef]

32. Steponavičienė, V.; Bogužas, V.; Sinkevičienė, A.; Skinulienė, L.; Vaisvalavičius, R.; Sinkevičius, A. Soil Water Capacity, Pore Size Distribution, and CO$_2$ Emission in Different Soil Tillage Systems and Straw Retention. *Plants* **2022**, *11*, 614. [CrossRef]
33. Neilson, J.W.; Pepper, I.L. Soil Respiration as an Index of Soil Aeration. *Soil Sci. Soc. Am. J.* **1990**, *54*, 428–432. [CrossRef]
34. Toosi, E.R.; Kravchenko, A.N.; Guber, A.K.; Rivers, M.L. Pore characteristics regulate priming and fate of carbon from plant residue. *Soil Biol. Biochem.* **2017**, *113*, 219–230. [CrossRef]
35. Torbert, H.A.; Wood, C.W. Effects of soil compaction and water-filled pore space on soil microbial activity and N losses. *Commun. Soil Sci. Plant Anal.* **1992**, *23*, 1321–1331. [CrossRef]
36. Sang, J.; Lakshani, M.M.T.; Chamindu Deepagoda, T.K.K.; Shen, Y.; Li, Y. Drying and rewetting cycles increased soil carbon dioxide rather than nitrous oxide emissions: A meta-analysis. *J. Environ. Manag.* **2022**, *324*, 116391. [CrossRef] [PubMed]
37. Cook, F.J.; Orchard, V.A. Relationships between soil respiration and soil moisture. *Soil Biol. Biochem.* **2008**, *40*, 1013–1018. [CrossRef]
38. Blagodatsky, S.; Smith, P. Soil physics meets soil biology: Towards better mechanistic prediction of greenhouse gas emissions from soil. *Soil Biol. Biochem.* **2012**, *47*, 78–92. [CrossRef]